Environ. Sci. Technol. **1998**, *32,* 1369−1377

Iso- and *Anteiso*-Alkanes: Specific Tracers of Environmental Tobacco Smoke in Indoor and Outdoor Particle-Size Distributed Urban Aerosols

ILIAS G. KAVOURAS, NIKOLAOS STRATIGAKIS, AND EURIPIDES G. STEPHANOU*

Environmental Chemical Processes Laboratory (ECPL), Division of Environmental and Analytical Chemistry, Department of Chemistry, University of Crete, 71409 Heraclion, Greece

Branched *iso*- and *anteiso*-alkanes were conjointly used, with *n*-alkanes and PAHs, as specific molecular markers to trace environmental tobacco smoke (ETS) in particle-sized aerosols collected in the indoor and outdoor urban atmosphere. GC/MS and GC-FID were used for the determination of *iso*-, *anteiso*-, and *n*-alkanes and PAHs. The branched alkanes (ranging from C_{29} to C_{33}) were detected only in particles in the accumulation range mode (<1.5 μm) in both indoor and outdoor samples. The concentrations of *iso*- and *anteiso*-alkanes in the indoor aerosols (0.75−8.53 ng/m^3) were higher than those measured in outdoor samples (0.77−1.51 ng/m^3). The indoor aerosol pattern of *iso*-, *anteiso*-, and their calculated diagnostic concentration ratios were characteristic for ETS. The compound distribution pattern of indoor *n*-alkanes (ranging from C_{21} to C_{33}) was of biogenic origin, and the use of odd-to-even predominance running ratio curves indicated their cigarette smoke origin. The corresponding outdoor pattern and concentration ratios, although less characteristic than the indoor ones, also indicated ETS as the main source of these compounds. The distribution study of the branched alkanes between gas and particulate phase in indoor aerosol demonstrated their presence only in the particles. On the other hand, PAHs in the gas phase gave a compound pattern more characteristic of ETS components than the PAHs present in the particulate phase. *Iso*- and *anteiso*-alkanes, due to their specificity, their nonreactive character, their association with the accumulation range mode particles, and therefore, their long atmospheric residence time, are the most suitable tracers for particulate ETS emissions in the indoor and outdoor urban atmosphere.

Introduction

Environmental tobacco smoke (ETS) is the material released into the ambient atmosphere by smoking tobacco products. Cigarettes are the primary concern because of their widespread use (e.g., 600 billion cigarettes are consumed in the United States per year) (*1*). Cigarette-generated ETS compounds derive primarily from side-stream smoke emitted between puffs and differ as the smoke mixture is diluted and aged.

Released reports (*1, 2*) include sufficient evidence to conclude that concerns about respiratory disease and the impairment of lung cancer development due to ETS exposure cannot be ruled out. Therefore, in the above-mentioned reports, research was required to determine the physical properties and chemical composition of ETS respirable suspended particulate matter (RSP), determining the gas-particulate phase distribution of ETS constituents and identifying suitable molecular markers for ETS exposure.

During the past decades, studies focusing on the gaseous and particulate smoke constituents have been conducted (*3*−*11*). The most important problem for environmental tobacco smoke indoor monitoring was to identify the correlation between ETS species and those compounds responsible for the observed human health effects (*1, 2*).

There are many factors for the selection of molecular markers or tracers of ETS. The knowledge of gas-to-particle distribution of the compounds is useful because of the different removal rates of each phase (*12*). On the other hand, indoor particles originating from ETS will be exchanged very rapidly with the outdoors, influencing the external particulate composition *(13*). Recently, researchers reported that cigarette smoke accounted for about 2.7% of the urban fine organic aerosol material (*14*). Therefore, appropriate molecular markers should be used to trace ETS presence outdoors as well.

Tracers of ETS used in the past include CO *(5*), nicotine *(5*), *N*-nitrosamines *(5, 6*), urinary concentrations of nicotine and cotinine *(5*), and sterols and sterenes (*9*). Nicotine is a unique gaseous compound and a major constituent of ETS. It could be a good biological marker as it metabolizes to cotinine. Cotinine is stable in the body, at detectable levels for several days (*9*). Nitrogen-containing compounds such as *N*-nitrosamine and 3-ethenylpyridine were also determined in several indoor environments in gaseous form (*4*−*7*). But the gas-to-particle distribution of nicotine and other nitrogen-containing compounds is a disadvantage to the suitability of these compounds as molecular tracers for ETS (*4, 5*).

RSP has been suggested as a potential tracer of ETS. However, RSP is emitted from several sources; therefore, it is neither specific for ETS nor representative for the exposure to the ETS gaseous constituents (*8*). PAHs are not source-specific and are susceptible to photodegradation in the atmospheric environment. Solanesol, a trisequiterpenoid alcohol ($C_{45}H_{74}O$), was also considered as a suitable particulate compound to trace ETS in the indoor environment (*10*). This compound is an alcohol with nine double bonds, and it was found to be very reactive under atmospheric conditions (e.g., O_3 and photooxidation). If the above-mentioned compounds are not the most appropriate ETS tracers for the indoor atmosphere, they are certainly not suitable for the same use in the outdoor environment.

2-Methyl- (*iso*-) and 3-methylalkanes (*anteiso*-alkanes) ranging from C_{29} to C_{34} had been proposed and successfully used as specific ETS tracers outdoors (*11, 14, 15*). These compounds show a characteristic concentration pattern in tobacco leaf surface wax and, consequently, in tobacco smoke, which is different from the one found in the leaf surface of other plants (*11*). In addition, none of these compounds was detected in crude oils as a result of diagenetic and catagenetic processes having occurred during oil formation (*11*). Therefore, *iso*- and *anteiso*-alkanes demonstrate

* To whom correspondence should be addressed; e-mail: stephanou@chemistry.uch.gr.

S0013-936X(97)00634-2 CCC: $15.00
Published on Web 04/08/1998

sufficient specificity and nonreactive character to be used as ETS tracers.

The objectives of this study were defined as follows: (a) the study of the presence of branched *iso*- and *anteiso*-alkanes conjointly with other ETS stable components such as *n*-alkanes and PAHs in indoor and outdoor size-distributed urban aerosols; (b) the investigation of the distribution of these compounds between the gas and particulate phase; and (c) the use of parameters such as Carbon Preference Index (CPI) (*16*), wax *n*-alkanes (WNA) content (*17*), "unresolved complex mixture" content to *n*-alkanes content (UCM/NA *(17)*), odd-to-even predominance (OEP) *(15, 18)*, and PAHs concentration diagnostic ratios *(15)* to reconcile the presence of *n*-alkanes and PAHs in particles and in the gaseous phase of indoor aerosols with ETS and to compare them with those from other possible emission sources. For the purpose of this study, urban aerosol samples were collected by using a five-stage (and backup) cascade impactor located in the interior and the exterior of a 20 m high building. Gaseous and particulate organic compounds were collected simultaneously by a high volume sampler containing a quartz filter followed by a polyurethane foam cartridge. In addition, samples were collected in a semi-urban and a rural location in order to check the presence, and thus the specificity, of *iso*- and *anteiso*-alkanes as tracers of ETS in the urban atmosphere.

Methodology

Site Characteristics and Sampling. All samples (29 in total) were collected in urban and nonurban locations on the Island of Crete in Greece. Six paired 12-h indoor and outdoor samples were simultaneously collected, with a high volume sampler, in two buildings (three samples indoors and three samples outdoors for each sampling site) and their surroundings, situated in the urban area of the city of Heraclion. Samples were collected in the main hall of the building of the University of Crete and in the main lobby of the State Telephone Company building. In both sites, smoking is allowed. Outdoor samples were collected on a seasonal basis (two additional samples were collected during rain). To assess the presence of ETS tracers in size-distributed air particles, two paired 24-h samples were collected indoors and outdoors of each building. Three simultaneous samplings of gas and particulate phase of ETS tracers were conducted in the lobby of the State Telephone Company building during working (two) and nonworking (one) hours. For comparison, the following samples were also collected: (a) two indoor samples in nonsmoking areas of the above-mentioned buildings, (b) three samples at a national road southwest of the city of Heraclion, and (c) three samples at the rural sampling station of the University of Crete, located on the northeastern coast of the Island of Crete *(15)*.

Sampling took place during 1994 (University building indoor and paired outdoor samples, one outdoor sample during rain) and 1995 (State Telephone Company building indoor and paired outdoor samples, one outdoor sample during rain, cascade impactor samples, sampling of gas and particulate phase, rural and semi-urban samples).

For sample collection, a high volume pump (GMWL-2000, General Metal Works, OH) was used. A pre-extracted 20 × 25 cm quartz fiber filter (Whatman, Maidstone, UK), having a collection efficiency higher than 99% for particles with radius larger than 0.3 μm at the 90 m^3/h flow rate used, was mounted on the high volume pump for the collection of urban, suburban, rural, and indoor total mass organic aerosols. For the size-distributed particles, a five-stage (plus backup filter) Sierra Andersen model 230 impactor was used mounted on the above-mentioned pump. Aerosol particles were separated into six size fractions on glass fiber filters according to the following equivalent cutoff diameters at 50% efficiency: first stage >7.2 μm, second stage 7.2−3.0 μm, third stage 3.0−1.5 μm, fourth stage 1.5−0.96 μm, fifth stage 0.96−0.5 μm, and backup filter <0.5 μm. Indoor gas and particulate phase were sampled as follows: Particles were sampled on a pre-extracted 120 mm diameter quartz fiber filter. Polyurethane foam plugs (PUF, 760 mm height and 610 mm diameter) placed downstream of the filter were used as adsorbents to trap vapor phase compounds at a 70 m^3/h flow rate. The filter and the PUF cartridge device were mounted on a Sierra Andersen model 1- PUF sampler. After collection, the filters were placed in glass tubes, and the PUF cartridges were wrapped in aluminum foil and stored in a freezer at −30 °C until extraction and analysis.

Materials. Solvents (SupraSolv grade) and standard compounds were purchased from Merck (Darmstadt, Germany). Silica gel (70−230 and 230−400 mesh) was also purchased from Merck (Darmstadt, Germany). Glass and quartz fiber filters were delivered by Whatman (Maidstone, UK). PUF cartridges were provided by Sierra Andersen. All materials were pre-extracted in a Soxhlet apparatus overnight and kept dry until use. Quartz filters were baked at 550 °C for 4 h and then kept in a dedicated clean glass container, with silica gel, to avoid humidity and contamination.

Fractionation, Derivatization, and Identification. A detailed description of the analytical procedure used for extraction, separation, and analysis of the main lipid fractions has been published elsewhere (*19*). The above protocol was applied for the determination of normal and branched alkanes in a composite tobacco sample from cigarette brands widespread in Greece. The separated organic compounds were analyzed by high-resolution gas chromatography and gas chromatography−mass spectrometry in the electron impact mode.

Calculations. (a) The wax *n*-alkanes concentration (WNA) was calculated as follows:

$$\text{wax } C_n = C_n - 0.5[(C_{n+1}) + (C_{n-1})]$$

Negative values of C_n were taken as zero.

(b) The odd Carbon Preference Indices (CPI) for *n*-alkanes were calculated as follows:

$$\text{CPI} = \sum C_{13}{-}C_{35} \Big/ \sum C_{12}{-}C_{34}$$

(c) Running OEP ratios were computed using the following equation:

$$\text{OEP for } C_n = [(C_{n-2} + 6C_n + C_{n+2})/(4C_{n-1} + 4C_{n+1})]^{(-1)^{(n-1)}}$$

OEP values were plotted vs the carbon chain length to construct the OEP curves.

(d) Dry deposition was calculated by the six-step method *(12, 20)*:

$$F_6 = \sum_{i=1}^{6} C_i V_d(D_i)$$

F_6 is the dry deposition flux (μg m^{-2} yr^{-1}), D_i is the midpoint cutoff diameter of each impactor stage (μm), V_d is the deposition velocity for each midpoint diameter particle (cm/s), and C_i is the concentration of hydrocarbons in each stage (ng/m^3).

(e) Wet deposition was evaluated according to the following model *(12, 21)*:

$$F = W_p P C_p$$

W_p is the washout factor, P is the annual precipitation (cm/

TABLE 1. Total Suspended Particle (TSP) and Total Solvent Organic Extract (TSOE) Concentration[a]

compd classes	urban aerosols	suburban aerosols	rural aerosols	indoor aerosols: nonsmoking area	indoor aerosols: smoking area	indoor gas-to-particle distribution: particles	indoor gas-to-particle distribution: gas phase	cigarette smoke[b]
TSP (μg/m^3)	85.00−93.00	26.30−122.60	12.95−31.95	0.89−31.10	155.10−774.40			
TSOE (μg/m^3)	6.20−14.80	1.10−1.80	1.73−3.03	0.15−3.64	37.1−516.3			
TSOE/TSP (%)	6.80−15.94	0.88−5.10	9.50−13.40	11.69−16.67	23.92−66.67			
				Aliphatics				
(C_m−C_n); $C_{n\ max}$	(C_{12}−C_{33}); C_{25}, C_{29}	(C_{12}−C_{33}); C_{25}	(C_{12}−C_{38}); C_{31}	(C_{17}−C_{34}); C_{31}	(C_{15}−C_{34}); C_{31}	(C_{14}−C_{33}); C_{25}, C_{27}	(C_{15}−C_{30}); C_{20}, C_{21}	(C_{21}−C_{35}); C_{31}
concn (ng/m^3)	65.0−320.0	7.8−17.8	2.28−16.05	5.23−7.15	371.6−2789.6	25.7−41.5	32.5−44.5	549.0
CPI	1.41 ± 0.18	1.66 ± 0.29	4.53 ± 1.10	1.75−1.84	3.09 ± 0.25	1.55 ± 0.35	0.91 ± 0.09	3.44
concn (branched)	4.5−13.48	nd	nd	0.72−0.99	217.71−1952.19	3.11−8.86	nd	289.2
branched-$C_{n\ max}$	*i*-C_{31}, *a*-C_{32}			*i*-C_{31}	*i*-C_{31}	*i*-C_{31}		*i*-C_{31}, *a*-C_{32}
UCM/NA	8.63−14.02	2.83−4.47	3.06−9.77	80.10−90.41	1.96−2.12	1.10−4.26	9.10−21.37	
WNA (%); $C_{n\ max}$	13.9−25.0; C_{25}, C_{29}	13.1−36.3; C_{25}	54.6−71.6; C_{31}	30.3−35.8; C_{31}	54.3−69.6; C_{31}	19.1−34.9; C_{27}, C_{31}	11.7−15.3; C_{20} .C_{21}	63.35; C_{31}
				PAHs				
TPAHs (ng/m^3)	20.0−60.0	0.17−1.14	0.1−2.8	0.002	21.0−1545.9	0.55−6.5	8.37−28.08	13.5
CPAHs/TPAHs	0.45 ± 0.04	0.42 ± 0.10	0.75 ± 0.10	0.08	0.70 ± 0.07	0.43 ± 0.17	0.17 ± 0.07	0.21
MP/P	3.20 ± 0.55	3.53 ± 1.75	0.98 ± 0.01	3.57	2.94 ± 1.02	2.64 ± 1.50	1.25 ± 0.15	
BA/BA+CT	0.34 ± 0.02	0.31 ± 0.09	0.20 ± 0.09		0.19 ± 0.01	0.17 ± 0.03	0.27 ± 0.09	0.28
BeP/BeP+BaP	0.70 ± 0.02	0.73 ± 0.15	0.79 ± 0.09		0.64 ± 0.09	0.34 ± 0.13		
Fl/Fl+Py	0.45 ± 0.06	0.54 ± 0.17	0.75 ± 0.11	0.61	0.34	0.46 ± 0.03	0.48 ± 0.03	0.48
IP/IP+BgP	0.30 ± 0.02	0.59 ± 0.27	0.61 ± 0.04		0.34	0.65 ± 0.14		

[a] Homologue ranges (C_m−C_n) and homologues with the maximum concentration ($C_{n\ max}$) for *n*- and branched alkanes. Concentration ranges for *n*- and branched alkanes and PAHs. Diagnostic molecular parameters for urban, suburban, rural, indoor aerosol, indoor gas and particulate phase, and cigarette smoke. UCM, unresolved complex mixture. NA, total *n*-alkanes. WNA, leaf wax *n*-alkanes. TPAHs, total PAHs concentration. CPAHs, combustion-derived PAHs. MP/P, methylphenanthre to phenanthrene. BA/BA+CT, benz[*a*]anthracene to [benz[*a*]anthracene + chrysene,-tryphenylene]. BeP/BeP+BaP, benzo[*e*]pyrene to [benzo[*e*]pyrene + benzo[*a*]pyrene]. Fl/Fl+Py, fluoranthene to [fluoranthene + pyrene]. IP/IP+BgP, indeno[1,2,3-*cd*]pyrene to [benzo[*ghi*]perylene + indeno[1,2,3-*cd*]pyrene]. [b] Concentrations are in μg/g.

yr), and C_p is the concentration of hydrocarbons on particles (ng/m^3). We used an annual precipitation value of 25 cm/yr for the Eastern Mediterranean and a washout factor of 10^5 for alkanes (*12*).

Results and Discussion

Samples General Characteristics. Concentrations of total suspended particles (TSP) and total solvent organic extract (TSOE) of the aerosol samples are given in Table 1. Also in Table 1 are reported for aliphatic compounds the concentration ranges for *n*- and branched alkanes, the homologue with the highest concentration ($C_{n\ max}$), the diagnostic molecular parameters such as Carbon Preference Index (CPI), and the wax *n*-alkanes content (WNA); for PAHs, the concentration range and the diagnostic concentration ratios of specific PAHs are given.

Higher TSP concentration levels (155.1−774.4 μg/m^3) were found in the indoor samples collected in smoking areas than in indoor nonsmoking areas (0.89−31.1 0 μg/m^3) and in urban (85.0−93.0 μg/m^3), suburban (26.3−122.6 μg/m^3), and rural (13.0−32.0 μg/m^3) areas (Table 1). The indoor concentration levels were affected by the sampling time period as well as by the number of people assembled in the sampling site, and they changed dramatically with the time of the day. The same was observed with the TSOE concentration levels. TSOE represented a lower amount of TSP in urban (7.0−17.0%), suburban (1.0−5.1%), rural (9.5−13.0%), and indoor nonsmoking areas (11.7−16.7%) samples, but a substantially higher amount in the indoor samples collected in spaces where smoking was practiced (24.0−66.7%) (Table 1).

***n*-Alkanes and *Iso*- and *Anteiso*-Alkanes.** These compounds are preferentially found in tobacco leaf surface waxes (*11*). *Iso*- and *anteiso*-alkanes were identified by means of their mass spectra. As authentic standards were not available, cigarette tobacco samples were extracted, and their lipids were separated with the same analytical protocol used for aerosols. In Figure 1A is presented the total ion chromatogram of the aliphatic fraction of a cigarette tobacco extract. This chromatogram is almost identical with the corresponding chromatogram obtained from the aliphatic fraction of an indoor aerosol extract (Figure 2A,C). In Figure 1, panels B and D, are presented the mass spectra of 2-methyltriacontane (*iso*-C_{31}) determined in cigarette tobacco (Figure 1B) and aerosol (Figures 1D and 2C) samples. These spectra are identical and contain the typical fragmentation pattern ($M^{\bullet+} - [C_3H_7^{\bullet}]$, m/z 393) for this branched alkane. In Figure 1, panels C and E, are presented the corresponding mass spectra of 3-methylhentriacontane (*anteiso*-C_{32}) determined in cigarette tobacco (Figure 1C) and aerosol (Figures 1E and 2C) samples. These spectra are also identical and contain the typical fragmentation pattern ($M^{\bullet+} - [C_2H_5^{\bullet}]$, m/z 421) for this branched alkane. All *iso*- and *anteiso*-alkanes reported in this study have been identified by using this approach.

A stronger odd/even predominance, expressed by CPI, was observed in indoor samples collected in smoking areas (CPI 3.09 ± 0.25) than in the corresponding nonsmoking (CPI 1.75−1.84), urban (CPI 1.41 ± 0.18), and suburban (CPI 1.66 ± 0.29) ones (Table 1). The CPI values of *n*-alkanes associated with indoor particles approached those associated with rural particles (CPI 4.53 ± 1.10), where biogenic inputs (from epicuticular waxes of higher plants) predominate (*15*). To differentiate the biogenic from the petrogenic origin of *n*-alkanes, the concentrations of wax terrestrial *n*-alkanes (WNA) were calculated. The wax *n*-alkanes percentage (WNA%) in indoor smoking areas samples ranged from 54.3% to 69.0% (Table 1), and their distribution maximized at *n*-C_{31} (Table 1). These values are considerably higher than those obtained for indoor nonsmoking (30.30−35.80%), urban (14.0−25.0%), and suburban (13.2−36.4%) areas and approached the corresponding values for rural samples (55.0−72.0%). The indoor smoking areas particles and their associated *n*-alkane GC profiles (Figure 2A), CPI values, and

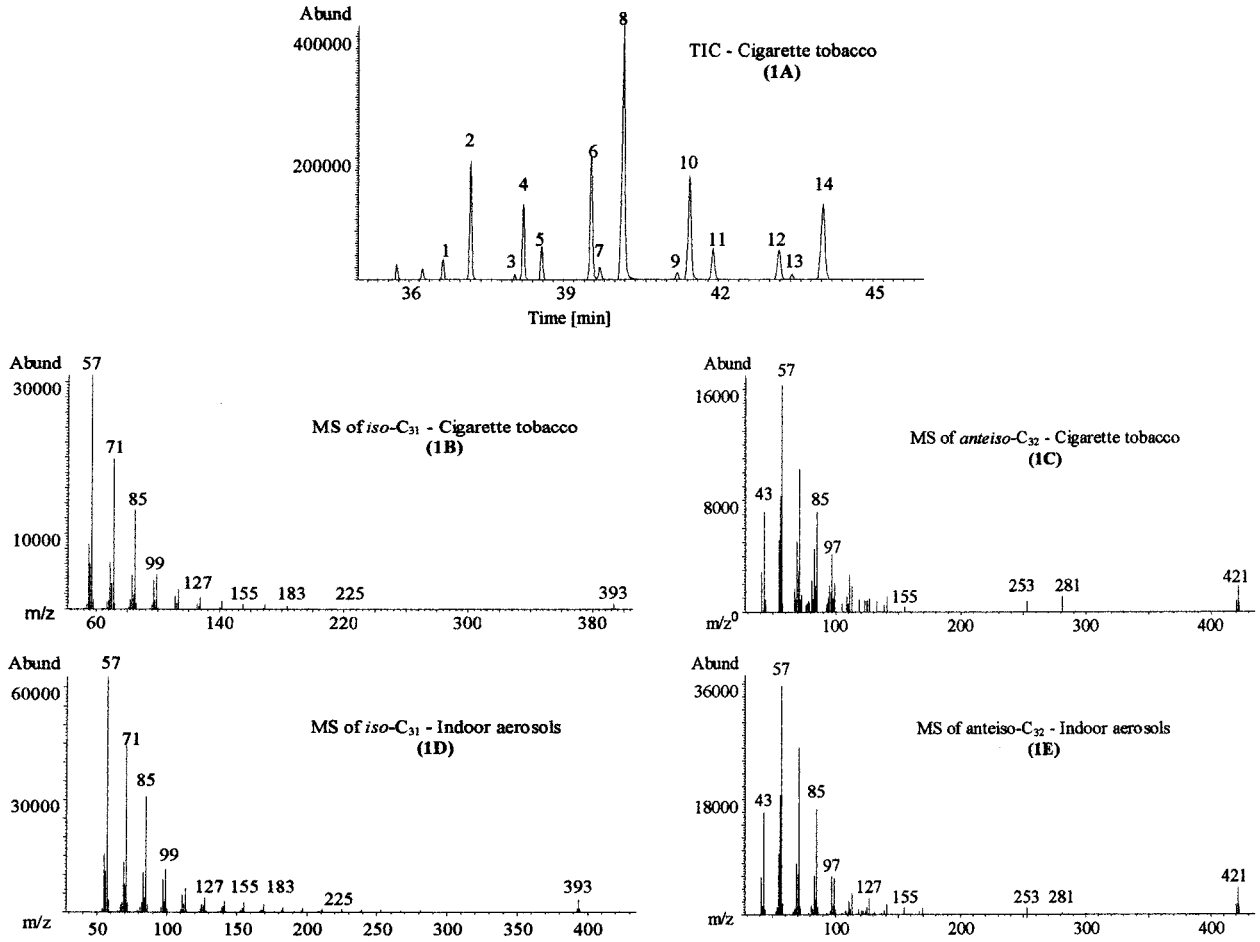

FIGURE 1. Segment of a total ion chromatogram (TIC, panel A) of the aliphatic fraction of cigarette tobacco extract. Mass spectra of *iso*-C_{31} (panel B) from cigarette tobacco extract (6, panel A), of *iso*-C_{31} from indoor aerosol extract (6, Figure 2C), of *anteiso*-C_{32} (panel C) from cigarette tobacco extract (10, panel A), of *anteiso*-C_{32} from indoor aerosol extract (10, Figure 2C). Compounds: (1) *i*-C_{29}, (2) *n*-C_{29}, (3) *i*-C_{30}, (4) *a*-C_{30}, (5) *n*-C_{30}, (6) *i*-C_{31}, (7) *a*-C_{31}, (8) *n*-C_{31}, (9) *i*-C_{32}, (10) *a*-C_{32}, (11) *n*-C_{32}, (12) *i*-C_{33}, (13) *a*-C_{33}, and (14) *n*-C_{33}.

WNA percentages (Table 1) had characteristics of a strong input of biogenic *n*-alkanes (*15*).

The daily *n*-alkanes particulate phase total concentration ranged from 25.76 to 41.55 ng/m^3 at the State Telephone Company Building indoor sampling site. Particle associated *n*-alkanes are dominated by the biogenic *n*-C_{27}, *n*-C_{29}, and *n*-C_{31} hydrocarbons (Figure 2A). These concentrations are comparable with those determined in the simultaneously collected gas phase, which ranged from 32.58 to 44.51 ng/m^3. The low molecular weight *n*-C_{19}, *n*-C_{20}, *n*-C_{21}, and *n*-C_{22} hydrocarbons are the dominant homologues in the gas phase (Figure 2B). Gas phase *n*-alkanes had CPI values lower than one (0.91 ± 0.09), high UCM/NA ratios (9.10−21.37), and low WNA percentages (11.69−15.30) (Table 1). The stronger biogenic character of particulate *n*-alkanes, in comparison to the gaseous ones, was also demonstrated by the higher CPI values (1.55 ± 0.31), the lower UCM/NA values (1.10−4.26), and the higher WNA percentages (19.12−34.94) (Table 1). Smoking intensity clearly influenced the extent of the parameters indicating the biogenic origin of *n*-alkanes in indoor samples. *Iso*- and *anteiso*-alkanes *(11, 14, 15)*, used to trace cigarette smoke, were considered in order to correlate their presence to the biogenic character of *n*-alkanes and to check if the strong biogenic indoor *n*-alkanes character is related with ETS. These branched aliphatic compounds are abundant in cigarette smoke particles and show a concentration pattern characteristic of tobacco leaf surface waxes (*11*). It is noteworthy that the branched *iso*- and *anteiso*-alkanes were absent in the gaseous phase while present in the particulate phase in concentrations ranging from 3.11 to 8.86 ng/m^3 (Figure 2A−C and Table 1). The presence of ETS-derived *iso*- and *anteiso*-alkanes only in the particulate phase shows that these compounds are, in addition to their chemical stability, suitable tracers for the particulate phase of ETS. The relative concentration distributions of *iso*- and *anteiso*-alkanes determined in indoor samples (Figure 3A) are convincingly similar to their distribution determined in cigarette smoke particles (Figure 3B) (*11*). The OEP curves calculated for *n*-alkane concentrations associated with indoor particles from a heavy smoking atmosphere (In1) and indoor particles separated from the gas phase (In2) and those calculated for *n*-alkanes in cigarette smoke (from *n*-alkane concentrations given in ref *11*) have almost identical shapes (Figure 4A). Thus, they further support the biogenic character of indoor *n*-alkanes with ETS. This observation jointly with the presence of *iso*- and *anteiso*-alkanes demonstrates the predominant input of *n*-alkanes, from cigarette smoke, in the indoor samples studied. For comparison purposes, the same curves were used to characterize *n*-alkanes associated with urban, suburban, and rural samples. Their representative OEP curves are shown in Figure 4C. It is obvious that plots of OEP versus *n*-alkane chain length vary among unrelated particle extracts, but they are similar for samples of common origin.

Characteristic *m/z* 85 + 99 mass chromatograms for indoor and outdoor urban aerosol samples are shown in Figure 2C,D. In the chromatogram of the outdoor sample, the presence of *iso*- and *anteiso*-alkanes is clearly demonstrated. In Table 2 are given diagnostic ratios of concentrations of *iso*- and *anteiso*-alkanes measured in indoor and

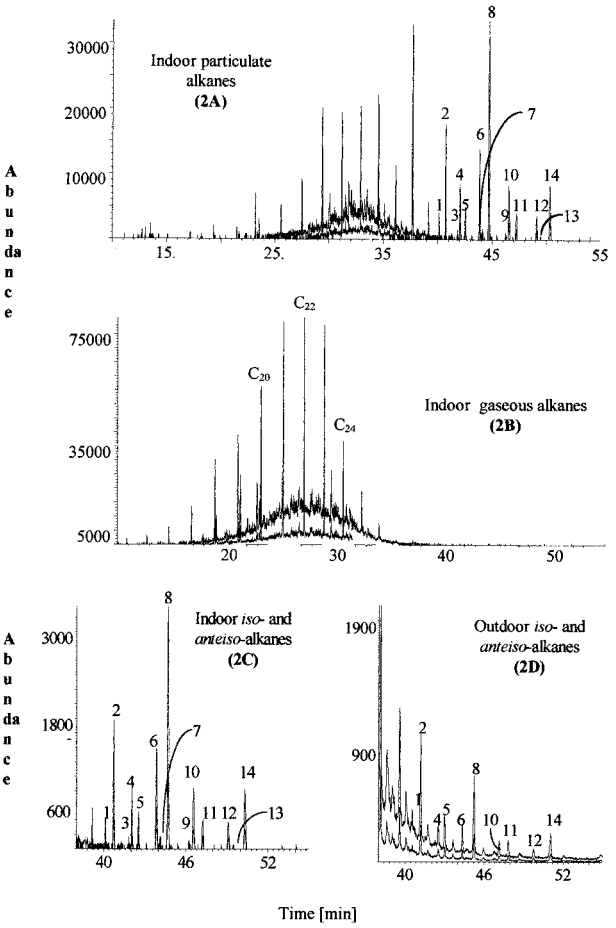

FIGURE 2. *n*-Alkane *m/z* 85 and 99 ion chromatograms for indoor particles (panel A) and gas phase (panel B). Segment of *m/z* 85 and 99 ion chromatograms for indoor (panel C) and outdoor (panel D) aerosols. Compounds: (1) *i*-C_{29}, (2) *n*-C_{29}, (3) *i*-C_{30}, (4) *a*-C_{30}, (5) *n*-C_{30}, (6) *i*-C_{31}, (7) *a*-C_{31}, (8) *n*-C_{31}, (9) *i*-C_{32}, (10) *a*-C_{32}, (11) *n*-C_{32}, (12) *i*-C_{33}, (13) *a*-C_{33} and (14) *n*-C_{33}.

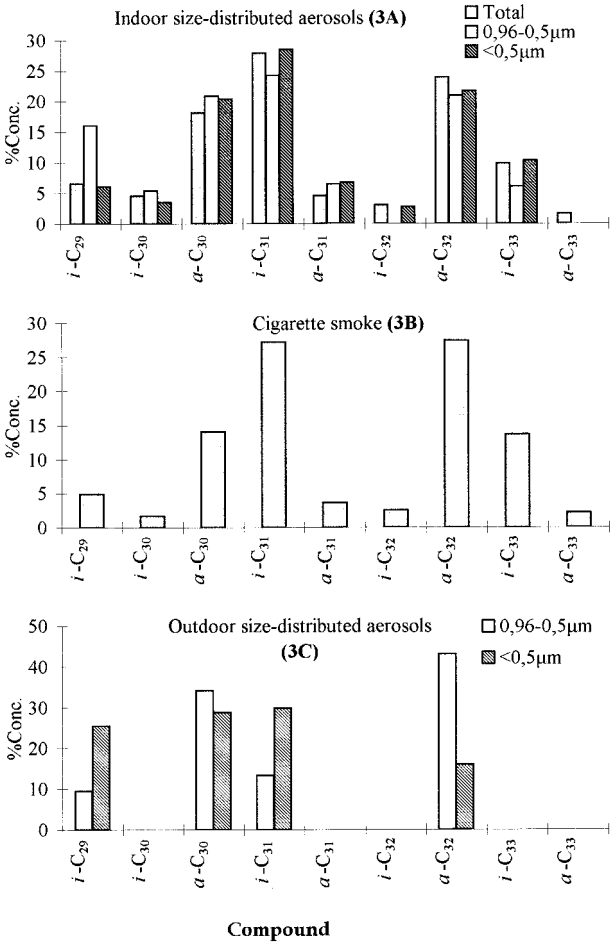

FIGURE 3. Relative concentration pattern of *iso*- (*i*-C_n) and *anteiso*-alkanes (*a*-C_n) in total and size-distributed (0.96−0.5 and <0.5 μm) indoor aerosol (panel A), cigarette smoke (panel B), and size-distributed (0.96−0.5 and <0.5 μm) outdoor aerosol (panel C).

outdoor samples examined in this study. By comparing the results obtained in this study and those published for cigarette tobacco, cigarette smoke, and leaf waxes (*11*), we can confirm that cigarette smoking is a source of aliphatic hydrocarbons also to the urban outdoor atmosphere. The ratios of concentrations of the most abundant *n*-, *iso*-, and *anteiso*-alkanes indicated that the *iso*- and *anteiso*-alkanes found in the urban atmosphere originate likewise from cigarette smoke. The concentration ratio of *anteiso*-C_{30} to *n*-C_{30} (*a*-C_{30}/*n*-C_{30}, Table 2) is 0.045 for leaf abrasion products, 2.24 for cigarette tobacco, and 1.71 for cigarette smoke. This pronounced difference is also reflected in indoor aerosol samples and in samples where the particulate phase was separated from the gaseous one (Table 2). A pronounced variation is also noticed in the concentration ratios of the following: *iso*-C_{31} to *n*-C_{31} (*i*-C_{31}/*n*-C_{31}, Table 2), which is 0.007 for leaf abrasion products, 0.41 for cigarette tobacco, 0.39 for cigarette smoke, 0.50−0.58 for indoor samples, and 0.12−0.58 for outdoor samples; *anteiso*-C_{32} to *n*-C_{32} (*a*-C_{32}/*n*-C_{32}, Table 2), which is 0.056 for leaf abrasion products, 3.17 for cigarette tobacco, 2.07 for cigarette smoke, 2.58−2.63 for indoor samples, and 0.66−1.94 for outdoor samples; *iso*-C_{33} to *n*-C_{33} (*i*-C_{33}/*n*-C_{33}, Table 2), which is 0.027 for leaf abrasion products, 0.35 for cigarette tobacco, 0.39 for cigarette smoke, 0.51−0.52 for indoor samples, and 0.08−0.43 for outdoor samples; *iso*-C_{33} to *iso*-C_{31} (*i*-C_{33}/*i*-C_{31}, Table 2), which is 1.87 for leaf abrasion products, 0.35 for cigarette tobacco, 0.50 for cigarette smoke, 0.25−0.35 for indoor samples, and 0.23−0.30 for outdoor samples; *anteiso*-C_{32} to *iso*-C_{33} (*a*-C_{32}/*i*-C_{33}, Table 2), which is 0.35 for leaf abrasion products, 2.95 for cigarette tobacco, 2.00 for cigarette smoke, 2.43−2.67 for indoor samples, and 1.45−2.84 for outdoor samples. Furthemore, if we assume that the presence of the most abundant *iso*- and *anteiso*-alkanes (*anteiso*-C_{30}, *iso*-C_{31}, *anteiso*-C_{32}, and *iso*-C_{33}, Table 2) found in our outdoor samples was due mostly to the leaf surface abrasion products, then the sum of their concentration could be used to calculate the expected concentrations of the corresponding *n*-alkanes (*n*-C_{30}, *n*-C_{31}, *n*-C_{33}, and *n*-C_{33}) by using the ratio of the summed concentrations of *iso*- and *anteiso*-alkanes ($\sum(i+a)C_n$) to the sum of concentrations of *n*-alkanes [$\sum nC_n$, calculated from data concerning leaf abrasion products (*11*), Table 2]. The estimated *n*-alkane concentrations should be 10−30-fold higher than those actually determined in this study (Table 2). This similarity of *iso*- and *anteiso*-alkanes aerosol distribution with the corresponding one of indoor aerosol (Table 2) implies that these branched alkanes originate from tobacco smoke. Comparable results were published for the Los Angeles urban area. *Iso*- and *anteiso*-alkanes were not detected in suburban and rural samples, pointing out that their presence is rather characteristic of the urban atmosphere.

Polycyclic Aromatic Hydrocarbons: Composition and Characteristics. Figure 5A shows the PAHs distribution in different urban, suburban, and rural aerosol samples. In Figure 5B are given the corresponding PAHs distributions indoors in the gas and the particulate phases. Collective

TABLE 2. Diagnostic Concentration Ratio Values for Indoor and Outdoor Size-Distributed *iso*- and *anteiso*-Alkanes, Cigarette Tobacco, Leaf Wax, and Cigarette Smoke

	indoor		indoor			outdoor					
diagnostic ratio	gas phase	particles	total	0.96−0.5 μm	<0.5 μm	total	0.96−0.5 μm	<0.5 μm	cigarette tobacco	cigarette smoke*	leaf waxes*
a-C_{30}/*n*-C_{30}		1.42	1.87−2.03	2.01	1.79	0.35−0.83	0.48	0.24	2.24	1.71	0.045
i-C_{31}/*n*-C_{31}		0.51	0.50−0.58	0.42	0.43	0.12−0.58	0.09	0.12	0.41	0.39	0.007
a-C_{32}/*n*-C_{32}		1.94	2.58−2.63	2.20	2.59	0.66−1.94	1.76	0.19	3.17	2.07	0.056
i-C_{33}/*n*-C_{33}		0.41	0.51−0.52	0.37	0.47	0.08−0.43			0.35	0.39	0.027
a-C_{30}/*i*-C_{31}		0.63	0.63−0.65	0.86	0.72	0.38−1.42	2.57	0.96	0.52	0.52	0.30
i-C_{33}/*i*-C_{31}		0.32	0.25−0.35	0.25	0.36	0.23−0.30			0.35	0.50	1.87
a-C_{32}/*i*-C_{33}		2.66	2.43−2.67	3.43	2.10	1.45−2.84			2.95	2.00	0.35
$\sum(i+a)-C_n/\sum n-C_n$		0.72	0.82−0.90	0.76	0.76	0.13−0.40	0.31	0.16	0.68	0.66	0.02

[a] Data obtained from Rogge et al. (*26*).

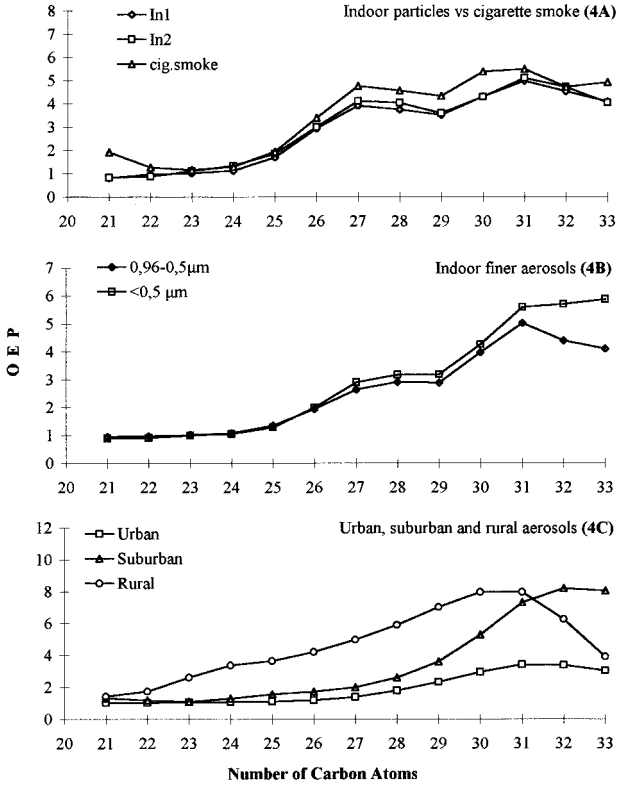

FIGURE 4. *n*-Alkane OEP plots for indoor aerosol (In1 and In2) cigarette smoke (panel A); size-distributed (0.96−0.5 and <0.5 μm) indoor aerosol (panel B); urban, suburban, and rural aerosol (panel C).

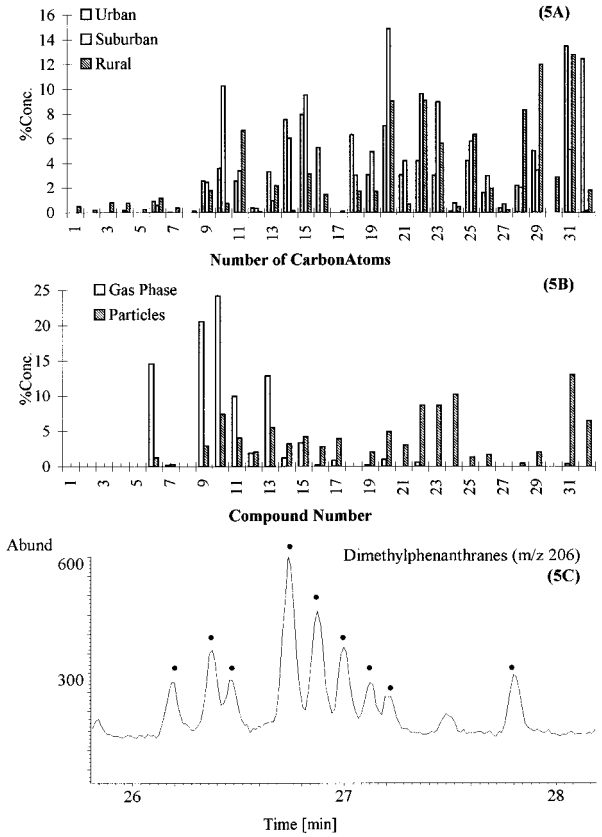

FIGURE 5. PAH relative compound distribution in urban, suburban, and rural aerosol (panel A); PAH relative compound distribution in indoor gas and particle phase (panel B). Dimethylphenanthrenes (●), *m/z* 206, ion chromatogram for indoor particles (panel C). Compounds: (1) naphthalene, (2) methylnaphthalene, (3) acenaphthane, (4) fluorene, (5) methylfluorene, (6) phenanthrane, (7) anthracene, (8) dimethylfluorene, (9) methylphenanthrane, (10) dimethylphenanthrane, (11) fluoranthene, (12) acephenanthrylene, (13) pyrene, (14) trimethylphenanthanes, (15) methylpyrene, (16) dimethylpyrene, (17) benzo[*ghi*]fluoranthene, (18) (4*H*)-cyclopenta-[*cd*]pyrene, (19) benz[*a*]anthracene, (20) chrysene/triphenylene, (21) methylchrysene/triphenylene, (22) benzo[*b/j*]fluoranthene, (23) benzo-[*k*]fluoranthene, (24) benzo[*a*]fluoranthene, (25) benzo[*e*]pyrene, (26) benzo[*a*]pyrene, (27) perylene, (28) indeno[7,1,2,3-*cdef*]chrysene, (29) indeno[1,2,3-*cd*]pyrene, (30) dibenz[*a,h*]anthracene, (31) benzo[*ghi*]-perylene, (32) coronene.

parameters and PAHs concentrations diagnostic ratios are given in Table 1.

Urban samples had total PAH concentrations (TPAHs) 2 orders of magnitude higher than those of the suburban and rural samples (Table 1) and 2 orders of magnitude lower than those of indoor samples collected during heavy smoking (Table 1). Although the qualitative composition of PAHs in all samples is very similar, the relative abundance of specific components within mixtures displays discernible differences. For example, urban samples contain mostly three- and four-ring compounds and their methylated derivatives (Figure 5A). Benzo[*ghi*]perylene and coronene are the most abundant components in all urban aerosol samples. Indoor aerosol samples contained fewer PAH compounds and had different compound distributions than urban and rural samples, with chrysene (+triphenylene), benzo[*e*]pyrene, and benzo[*ghi*]perylene being the most abundant homologues. In addition, the examination of the relative concentrations of dimethylphenanthrene (DMP) isomers (Figure 5C) indicated that indoor air particulate matter present the same DMP isomers pattern as samples originating from motor vehicle emissions (*22*).

Urban samples are characterized by a relative value stability of these ratios (Table 1). The sum of concentrations of nine major nonalkylated compounds (fluoranthene,

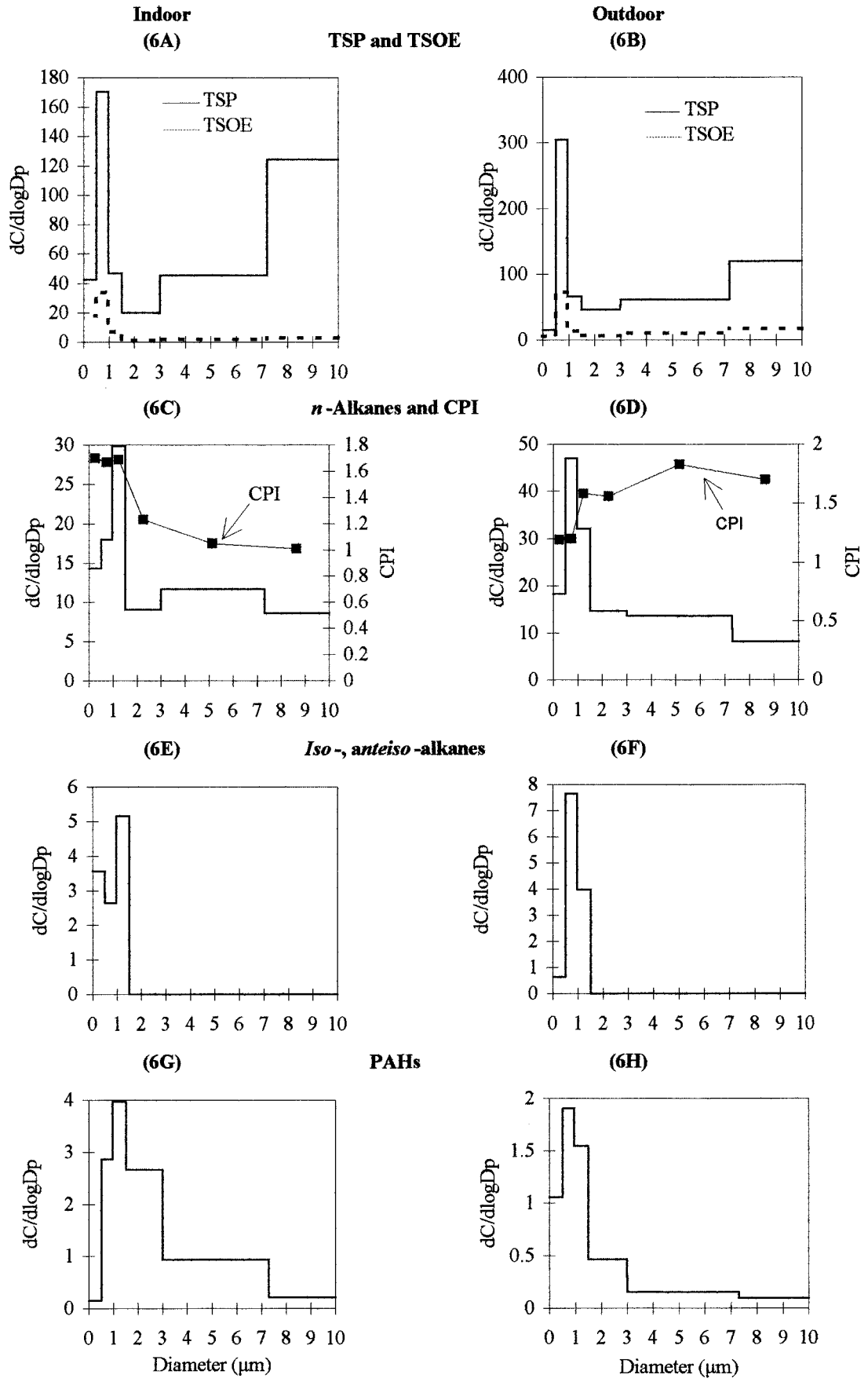

FIGURE 6. Lundgren diagrams for indoor and outdoor total suspended particles (TSP), total solvent organic extract (TSOE) (panels A and B), *n*-alkanes (panels C and D), *iso*- and *anteiso*-alkanes (panels E and F), and PAHs (panels G and H), concentration.

TABLE 3. Size-Distributed Concentration and Calculated Dry and Wet Deposition Fluxes of *iso*-C_{31} and *n*-C_{31} from Cascade Impactor Measurement Data

			iso-C_{31}			*n*-C_{31}		
diameter (μm)	V_d (cm s^{-1})	W_p	concn (ng m^{-3})	flux of dry deposition (μg m^{-2} yr^{-1})	flux of wet deposition (μg m^{-2} yr^{-1})	concn (ng m^{-3})	flux of dry deposition (μg m^{-2} yr^{-1})	flux of wet deposition (μg m^{-2} yr^{-1})
>7.2	2.000	10^5			0.00	0.78	491.96	19.50
7.2−3.0	0.300	10^5			0.00	0.85	80.42	21.25
3.0−1.5	0.030	10^5			0.00	0.61	5.77	15.25
1.5−0.96	0.010	10^5	0.33	1.04	8.25	0.97	3.06	24.25
0.96−0.5	0.006	10^5	0.18	0.34	4.50	3.17	6.00	79.25
<0.5	0.070	10^5	2.43	53.64	60.75	3.66	80.80	91.50
total			2.94	55.02	73.50	10.04	668.00	251.00

pyrene, benz[*a*]anthracene, chrysene, benzofluoranthenes, benzo[*a*]pyrene, benzo[*e*]pyrene, indeno[*cd*]pyrene, and benzo[*ghi*]perylene), expressed as CPAHs, to the total concentration of PAHs [CPAHs/TPAHs *(23)*] had a mean value of 0.45 (±0.04) in urban samples and 0.70 (±0.07) in samples collected in smoking areas indoors. These values point out that in combustion the PAHs were the major components in indoor aerosols in comparison to urban and suburban ones, where petrogenic PAHs were more abundant. Significant differences were found in the concentration ratio of methylphenanthrenes to phenanthrene [MP/P, which has been used for source identification of PAHs *(23)*] of urban, suburban, and indoor samples in comparison to the rural ones (Table 1). The mean MP/P value of urban samples was 3.20 (±0.55), of suburban samples was 3.53 (±1.75), and of indoor samples was 2.94 (±1.02). These values characterize unburned fossil PAH mixtures connected to vehicular traffic *(23, 24)*. The MP/P values confirm the indications provided by the CPAHS/TPAHS values.

To further assess the different sources of PAHs present in the examined aerosol samples, a comparison (with caution) can be made between the diagnostic ratios benz[*a*]anthracene to [benz[*a*]anthracene + chrysene,tryphenylene] (BA/BA+CT), benzo[*e*]pyrene to [benzo[*e*]pyrene + benzo[*a*]pyrene] (BeP/BeP+BaP), fluoranthene to [fluoranthene + pyrene] (Fl/Fl+Py), and indeno[1,2,3-*cd*]pyrene to [benzo[*ghi*]perylene + indeno[1,2,3-*cd*]pyrene] (IP/IP+BgP), which are usually used for source reconciliation *(24−26)*. The comparison of the above values with the corresponding ones obtained in indoor particles and cigarette smoke from the outdoor atmosphere and ETS (Table 1) indicated that these particles have, with respect to their PAHs composition, a rather mixed origin. When the gaseous phase was simultaneously collected with the particulate, the following observations were made: PAH concentrations ranged from 8.37 to 28.08 ng/m^3 in the gas phase and from 0.55 to 6.5 ng/m^3 in the particulate phase. Their composition differs greatly (Figure 5B). The above-mentioned diagnostic ratios of concentrations of particular PAHs indicate that the gaseous PAHs found in the indoor atmosphere originate mostly from cigarette smoke. The ratio CPAHS/TPAHS for gas-phase associated PAHs is 0.17 ± 0.07, a value that is very close to the 0.21 value (Table 1) determined in cigarette smoke (*11*). The same is true for the ratios BA/BA+CT, 0.27 ± 0.09 (0.28 for cigarette smoke, Table 1), and Fl/Fl+Py, 0.48 ± 0.03 (0.48 for cigarette smoke, Table 1).

Particle-Size Distribution of *n*-Alkanes, Branched Alkanes, and PAHs Indoors and Outdoors. The relative concentration of *n*-alkanes, branched alkanes, and PAHs in total composition is strongly particle size dependent. This fact can be illustrated by using Lundgren plots (*27, 28*). Total concentrations of TSP, TSOE, *n*-alkanes, branched alkanes, and PAHs as a function of particle size for indoor and outdoor aerosols are shown in Figure 6. TSP diagrams (particularly in the indoor sample, Figure 6A) have a bimodal distribution.

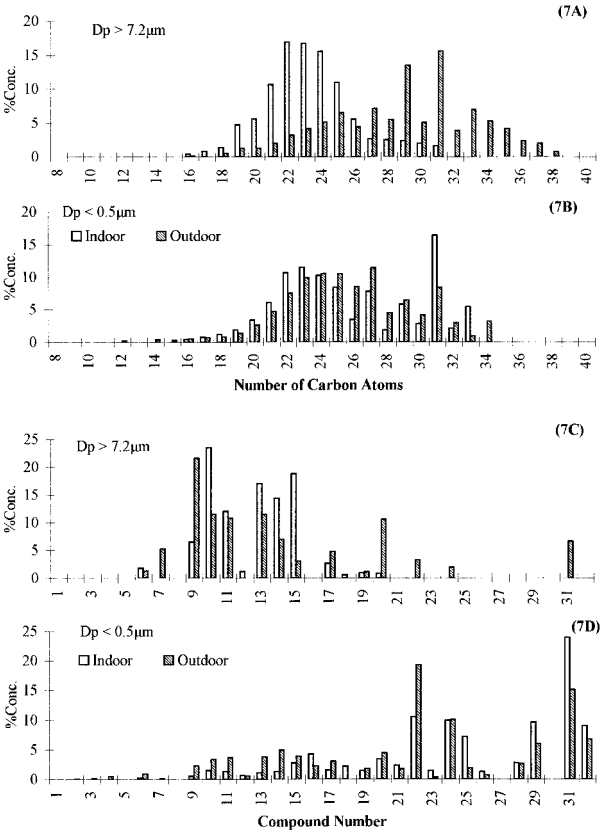

FIGURE 7. *n*-Alkane and PAH relative compounds distribution in coarser (Dp > 7.2 μm; panels A and C) and finer (Dp < 0.5 μm; panels B and D) indoor and outdoor aerosols.

On the other hand, TSOE plots (Figure 6A,B) exhibit a predominant occurrence of TSOE in the size fraction smaller than 1.5 μm. The same was observed for outdoor urban aerosols (*29*), where in quantitative terms *n*-alkanes and PAHs predominate in the submicron fractions (and chiefly the <0.5 μm fraction). Similar observations were made in our study for *n*-alkanes (Figure 6C,D) and PAHs (Figure 6G,H) of indoor and outdoor aerosols. Also plotted in Figure 6, panels C and D, are the CPI values for indoor and outdoor aerosols as a function of particle size. The decrease of CPI with particle size in outdoor aerosols (Figure 6D) strongly suggests an increasing contribution of petrogenic hydrocarbons in the aerosols containing smaller particles. This fact has also been previously reported *(29)*. In contrast to outdoor aerosols, for indoor aerosols CPI is increasing with particle size decrease (Figure 6C), showing that biogenic *n*-alkanes accumulate in the fine particles of the examined indoor sampling sites. In addition, the total concentration of *iso*- and *anteiso*-alkanes is accumulated in particles <1.5 μm. In

the fractions >1.5 μm *iso*- and *anteiso*-alkanes were not detected in either indoor (Figure 6E) or outdoor (Figure 6F) samples. The compound distribution of *iso*- and *anteiso*-alkanes in the small fractions of indoor aerosol (Figure 3A) has the same pattern as the distribution of these compounds in cigarette smoke (Figure 3B). Similarities are to be observed also in the corresponding compound distribution pattern of outdoor aerosol (Figure 3C).

Representative distributions of *n*-alkanes in coarser (>7.2 μm) and finer (<0.5 μm) aerosol fractions are shown in Figure 7, panels A and B. These *n*-alkane distributions show dominant concentrations between C_{17} and C_{36}. Coarser particles contain a higher relative proportion of homologues with higher molecular weights (>C_{26}) in the outdoor samples (Figure 7A). Conversely in indoor samples (Figure 7A) the coarser fractions contain a higher percentage of *n*-alkanes in the range of C_{17}−C_{27}. It is noteworthy that indoor *n*-alkane particle size distributions show a predominance of higher plant hydrocarbons C_{27}−C_{33} in the smallest particle size fraction (Figure 7B). OEP *n*-alkane plots (Figure 4B) show that the plot corresponding to particles collected on the backup filter is almost identical to that of cigarette smoke (Figure 4A). This observation demonstrates that the wax *n*-alkanes enrichment in the finer indoor aerosol fraction is due to ETS. In addition, diagnostic branched and *n*-alkane individual concentration ratios (*a*-C_{30}/*n*-C_{30}, *i*-C_{31}/*n*-C_{31}, *a*-C_{32}/*n*-C_{32}, *i*-C_{33}/*n*-C_{33}, *i*-C_{33}/*i*-C_{31}, and *a*-C_{32}/*i*-C_{33}; Table 2) associated with submicron particles (<0.5 μm) indoors are very similar to the corresponding ratios obtained for cigarette tobacco and cigarette smoke (Table 2 and ref *11*). The same ratios (Table 2) considered for the outdoor finer particle fraction are definitely closer (especially for particles in the range of 0.96−0.5 μm, Table 2) to the ratios for cigarette smoke than to those obtained for leaf waxes (Table 2, ref *11*).

Particle size distributions of PAHs in indoor and outdoor aerosols in coarser (>7.2 μm) and finer (<0.5 μm) aerosol fractions are also shown in Figure 7, panels C and D. Coarser particles in both indoor and outdoor samples contain mostly the petrogenic alkylated homologues (Figure 7C). On the contrary, the finer fraction is dominated by catacondensed structures of pyrolytic origin (Figure 7D).

Deposition Potential of *Iso*- and *Anteiso*-Alkanes. In Table 3 are presented the calculated results (see Methodology) for wet and dry deposition of branched and *n*-alkanes. For these calculations, we used data obtained from cascade impactor measurements. As we can notice, the most abundant biogenic alkane *n*-C_{31} concentration outdoors was highest (77.6% of the total concentration) in the fine aerosol (accumulation mode, 0.08 μm < *D* < 1.5 μm, Table 3). The *n*-C_{31} flux for dry deposition was calculated to be 668.0 μg m^{-2} yr^{-1} and for wet deposition was 251.0 μg m^{-2} yr^{-1} (Table 3). Coarse particles (>3 μm) contribute 66.7% to *n*-C_{31} total flux, denoting that total deposition of biogenic *n*-alkanes is dominated by coarse particles. In contrast, the most abundant branched alkane *iso*-C_{31} was associated only with the accumulation-mode particles (0.08 μm < *D* < 1.5 μm, Table 3). These accumulation-mode particles as compared with coarse particles are too small to undergo rapid gravitational settling, and they are more slowly removed by dry deposition. As a result, their atmospheric lifetimes are greater (*20*) (they can persist even more than 10 days), and consequently the *iso*- and *anteiso*-alkanes associated with them will have (due also to their chemical stability) longer atmospheric lifetimes than the corresponding *n*-alkanes. Wet deposition calculations showed (Table 3) that only 21.2% of *n*-C_{31} was deposited by rain scavenging of fine particles, while 57% of iso-C_{31} was deposited by the same process. As *iso*- and *anteiso*-alkanes were present only in the accumulation-mode particles, we expect them to be preferentially deposited by wet deposition. Indeed *iso*- and *anteiso*-alkanes were not determined in the urban atmosphere during the rain event.

Acknowledgments

The Special Research Account of the University of Crete is acknowledged for financial support.

Literature Cited

(1) *National Research Council. Environmental Tobacco Smoke. Measuring Exposure and Assessing Health Effects*; National Academy Press: Washington, DC, 1986.
(2) *The Health Consquences of Involuntary Smoking*; A report of the Surgeon General; U.S. Department of Health and Human Services, 1986.
(3) Eatough, D. J.; Benner, C. L.; Tang, H.; Landon, V.; Richards, G.; Caka, F. M.; Crawford, J.; Lamb, J. D. *Environ. Intl.* **1989**, *15*, 19−29.
(4) Odgen, M. W.; Maiolo, K. C. *Environ. Sci. Technol.* **1992**, *26*, 1226−1234.
(5) Eatough, D. J.; Benner, C. L.; Bayona, J. M.; Richards, G.; Lamb, J. D.; Lee, M. L.; Lewis, E. A.; Hansen, L. D. *Environ. Sci. Technol.* **1989**, *23*, 679−687.
(6) Hodgson, A. T.; Daisey, J. M.; Mahanama, K. P. R.; Ten Brinke, J.; Alevantis, L. E. *Environ. Int.* **1996**, *22*, 295−308.
(7) Kariyawasam, R.; Mahanama, K. P. R.; Daisey, J. M. *Environ. Sci. Technol.* **1996**, *30*, 1477−1485.
(8) Spengler, J. D.; Tretman, R. D.; Testeson, T. D.; Mage, D. T.; Soczek, M. L. *Environ. Sci. Technol.* **1985**, *19*, 700−707.
(9) Benner, C. L.; Bayona, J. M.; Caka, F. M.; Tang, H.; Lewis, L.; Crawford, J.; Lamb, J. D.; Lee, M. L.; Lewis, E. A.; Hansen, L. D.; Eatough, D. J. *Environ. Sci. Technol.* **1989**, *23*, 688−699.
(10) Tang, H.; Richards, G.; Benner, C. L.; Tuominen, J. P.; Lee, M. L.; Lewis, E. A.; Hansen, L. D.; Eatough, D. J. *Environ. Sci. Technol.* **1990**, *24*, 848−852.
(11) Rogge, W. F.; Hildemann, L. M.; Mazurek, M. A.; Cass, G. R.; Simoneit, B. R. T. *Environ. Sci. Technol.* **1994**, *28*, 1375−1388.
(12) Bidleman, T. F. *Environ. Sci. Technol.* **1988**, *22*, 361−367.
(13) Miguel, A. H.; De Aquino Neto, F. R.; Cardoso, J. N.; Vasconcellos, P. D. C.; Pereira, A. S.; Marquez K. S. G. *Environ. Sci. Technol.* **1995**, *29*, 338−345.
(14) Schauer, J. J.; Rogge, W. F.; Hildemann, L. M.; Mazurek, M. A.; Cass, G. R.; Simoneit, B. R. T. *Atmos. Environ.* **1996**, *22*, 3837−3855.
(15) Gogou, A.; Stratigakis, N.; Kanakidou, M.; Stephanou, E. G. *Org. Geochem.* **1996**, *25*, 79−96.
(16) Bray, E. E.; Evans, E. D. *Geochim. Cosmochim. Acta* **1961**, *22*, 2−15.
(17) Simoneit, B. R. T.; Cardoso, J. N.; Robinson, N. *Chemosphere* **1990**, *21*, 1285−1301.
(18) Scalan, R. S.; Smith J. E. *Geochim. Cosmochim. Acta* **1970**, *34*, 611−620.
(19) Stephanou, E. G.; Stratigakis, N. *J. Chromatogr.* **1993**, *644*, 141−151.
(20) Holsen, T.; Noll, K. E. *Environ. Sci. Technol.* **1992**, *26*, 1807−1815.
(21) Ligocki, M. P.; Leuenberger, C.; Pankow, J. F. *Atmos. Environ.* **1985**, *19*, 1619−1626.
(22) Benner, B. A.; Wise, S. A.; Currie, L. A.; Klouda, G. A.; Klinedinst, D. B.; Zweidinger, R. B.; Stevens, R. K.; Lweis, C. W. *Environ. Sci. Technol.* **1995**, *29*, 2382−2389.
(23) Takada, H.; Onda, T.; Ogura, N. *Environ. Sci. Technol.* **1990**, *24*, 1179−1186.
(24) Grimmer, G.; Hildebrandt, A. *Zbt. Bakt. Hyg. (I. Abt. Orig)* **1975**, *B161*, 104−124.
(25) Grimmer, G.; Jacob, J.; Naujack, K. W. *Fresenius J. Anal. Chem.* **1983**, *314*, 13−19.
(26) Rogge, W. F.; Hildemann, L. M.; Mazurek, M. A.; Cass, G. R.; Simoneit, B. R. T. *Environ. Sci. Technol.* **1993**, *27*, 636−651.
(27) Poster, D. L.; Hoff, R. M.; Baker, J. E. *Environ. Sci. Technol.* **1995**, *29*, 636−651.
(28) Aceves, M.; Grimalt, J. O. *Environ. Sci. Technol.* **1993**, *27*, 2896−2908.
(29) Sicre, M. A.; Marty, J. C.; Saliot A.; Aparicio, X.; Grimalt, J.; Albaiges, J. *Atmos. Environ.* **1987**, *21*, 2247−2259.

Received for review July 21, 1997. Revised manuscript received February 16, 1998. Accepted February 24, 1998.

ES970634E